V European Conference on Computational Fluid Dynamics
ECCOMAS CFD 2010
J. C. F. Pereira and A. Sequeira (Eds)
Lisbon, Portugal, 14–17 June 2010

THREE-PHASE NUMERICAL SIMULATION OF BLOOD FLOW IN THE ASCENDING AORTA WITH DISSECTION

G. Hou[*], K. Tsagakis[††], D. Wendt[††], S. Stühle[*], H. Jakob[††], W. Kowalczyk[*]

[*] Chair of Mechanics and Robotics, University of Duisburg-Essen
Lotharstr. 1, D-47057 Duisburg, Germany
e-mail: {guojun.hou, wojciech.kowalczyk}@uni-due.de

[††] Department of Thoracic and Cardiovascular Surgery, West-German Heart Center Essen, University Hospital Essen
Hufelandstr. 55, D-45122 Essen, Germany
{daniel.wendt, konstantinos.tsagakis, heinz.jakob}@uk-essen.de

Key words: Aortic Dissection, Computational Fluid Dynamics, Multiphase Flow, Blood Flow

Abstract. *Aortic dissection is one of the most life-threatening diseases of the human cardiovascular system. Since the fluid dynamic behavior of several blood elements in false and true lumen is not well understood so far, in this paper modeling and numerical simulations of the multiphase flow in the aorta without dissection as well as with dissections Stanford type A and B are presented. Additionally, influence of the biological heart valve prosthesis on the blood flow is shown. The blood is modeled as a multiphase medium that consists of three phases: plasma, red blood cells (RBCs) and leukocytes. The non-Newtonian behavior of the fluid depends not only on the shear rate but also on the volume fraction of RBCs. The numerical simulations are carried out with the RBC volume fraction of 38 % and 44 %. In order to model physiological conditions in the computational domain, a pulsatile flow with the maximum stroke volume of 70 ml and 120 ml is considered. The results reveal significant influence of the process parameters and the heart valve prosthesis on the blood flow characteristics and the hematocrit distribution in dissections and true lumen. The RBC distribution in the false lumen varies in a very wide range in the upper and the lower part of dissection. It is clearly seen that hematocrit has a tendency to separate from plasma as well as sediment and coagulate at the bottom of the false lumen.*

1 INTRODUCTION

The analysis of blood flow in the aorta belongs to experimental and numerical very intensive investigated fields of (bio-)fluid mechanics [1-6]. In the foreground of these investigations stay the research of very complex interactions between the blood flow patterns and the artery walls both in healthy and pathological vascular systems.

An aortic dissection is one of the most life-threatening diseases of the human vascular system [7]. Recently huge efforts are performed to increase the efficiency of medical treatment in this area [8-12]. In order to understand much better the fluid dynamic behavior of blood in aortic dissections, some theoretical and experimental works with one phase system are also carried out [13]. These investigations indicate significant influence of blood flow parameters on the hemodynamics in the true and false lumen. In particular, in the systole phase high velocity gradients in the false lumen are observed. Additionally, an essential pressure difference between the false and true lumen was seen. This pressure difference can contribute to further growth of false lumen and even rupture of the aorta. Thus, considering normal and shear strain distributions, an interesting behavior of multiphase systems in this range of geometry can be supposed.

This paper aims at the numerical simulations of blood flow in the ascending and descending aorta with dissections Stanford type A and B. An influence of the 3F-Enable heart valve prosthesis [14] on hemodynamics is also analyzed. These investigations focus on the study of the RBC volume fraction as well as the velocity patterns in the false and true lumen.

The results of the current paper contribute to knowledge about the fluid dynamic behavior of blood as a multiphase medium and thrombosis mechanisms in dissections.

2 METHODS

2.1 Governing equations

The numerical model is based on the Eulerian-Eulerian approach due to very high number of particles. It consist of the conservation equation of mass

$$\frac{\partial(\alpha_k \rho_k)}{\partial t} + \nabla \cdot \left(\rho_k \alpha_k \bar{u}_k\right) = 0 \tag{1}$$

and the conservation equation of momentum for multiphase system

$$\frac{\partial\left(\rho_k \alpha_k \bar{u}_k\right)}{\partial t} + \nabla \cdot \left(\rho_k (\alpha_k \bar{u}_k \otimes \bar{u}_k)\right) = \nabla \cdot \left(\mu_{eff,k} \alpha_k \left(\nabla \bar{u}_k + \left(\nabla \bar{u}_k\right)^T\right)\right) - \alpha_k \nabla p + \overline{M_{k,l}} \,. \tag{2}$$

The last term in Eq. 2 denotes the total interfacial momentum between the dispersed and continuous phase including the sum of the drug, lift, buoyancy and virtual forces [15].

2.2 Numerical model

The numerical simulations are realized using an Eulerian-Eulerian multiphase model. The blood is considered as a multiphase substance that consist of plasma, red blood cells (RBCs) and leukocytes. In this paper following volume fractions for each of these components are applied: plasma 61 % and 55 %, RBCs 38% and 44 % and leukocytes 1 %. These two values of RBCs can be associated with common observed gender differences. The plasma is modeled as a continuous Newtonian fluid with the constant viscosity of 0.001 [Pa s] and the density of 1003 [kg/m^3]. RBCs are taken as a spherical dispersed phase with the diameter of 8 µm and the density of 1080 [kg/m^3]. The

transport properties of hematocrit depend on both the shear rate and the RBC volume fraction. Additionally, the fluid dynamic behavior of leukocytes, as a dispersed phase that contains spherical particles with the diameter of 18 µm and the density of 1064 [kg/m^3] is modeled. Details of the viscosity modeling can be seen in [16].

Since blood flow in the aorta can reach Re number of 10^3, the modeling of turbulence effect is performed. The algebraic model Dispersed Phase Zero Equation [15] is taken for dispersed phase while the Shear Stress Transport (SST) model is applied for modeling the turbulence in the continuous phase [17].

Four different computational domains (see Fig. 1) are created with ANSYS ICEM CFD (ANSYS, Inc.). The inner diameter of the aorta amounts 25 mm. The entries to the false lumen of the dissection A and B have an elliptic form with a major and minor axis of 6 mm and 3 mm respectively.

Unstructured mesh of approx. 500.000 tetrahedral elements is generated for the computational domains without the heart valve prosthesis. In the geometry with the dissection type B and the heart valve prosthesis, 1.1 million elements are created. The three dimensional simulation of the fluid flow in the aorta is carried out with the finite volume method implemented within ANSYS CFX 12.0 (ANSYS, Inc.). Using adaptive time stepping method, the initial time step is set to 5e-4 [s], whereby the minimum and maximum time step lie in the range between 5e-5 [s] and 1e-2 [s]. The increase and decrease of the time step occurs after 5 target loops with the factor of 1.06 and 0.8. The maximum time step is reached after 0.17 [s] for all cases. The standard calculation is case dependent and takes a CPU time from 8 to 58 hours on a serial workstation (Pentium Q9300, 2.5 GHz, 4 GB RAM).

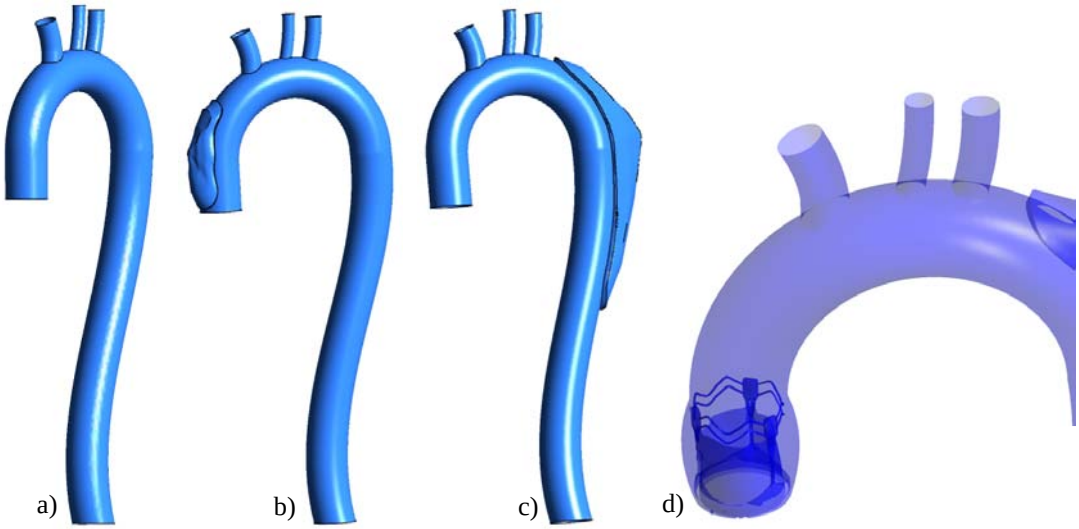

Figure 1: The computational domains of the aorta: a) without dissection, b) dissection Stanford type A, c) dissection Stanford type B and d) dissection Stanford type B as in c) and additionally with the heart valve prosthesis.

The numerical simulations are carried out within two stages. As first, steady state calculations with the maximal stroke volumes are performed. In dependence on the case, the convergence criteria of RMS 1e-4 are reached after 40-60 iterations. Afterwards, transient numerical simulations of the pulsatile flow are realized. The results from the steady state calculations are inserted as initial conditions. In order to model physiological conditions in the computational domain, a pulsatile flow with the maximum stroke volume of 70 ml and 120 ml is considered. The transient simulations consider 5 pulsatile cycles realized within 5 s. The boundary condition applied at the inlet of the aorta is shown in Fig. 2. At the outlet the opening boundary condition with

zero gradient condition for all phases is applied. To simulate physiological conditions in the carotid arteries, the continuous flow volume of blood in the range of 5 % [18] of the complete blood volume applied at the inlet is used.

Since the leukocyte volume fraction is approx. 1 % and no significant influence on blood flow has been observed during preliminary calculations, the results from two phase flow simulations are analyzed in details. Nevertheless, to deliver new cognitions for bio-chemical and medical applications complete three phase blood flow will be evaluated in further studies.

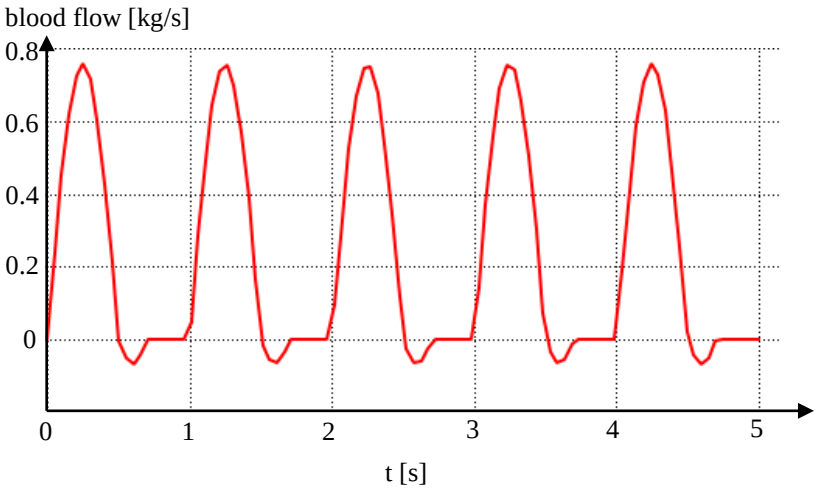

Figure 2: The blood flow applied at the inlet of the aorta for the case with the stroke volume of 70 ml. In the case with the stroke volume 120 ml the ordinate is scaled up to 0.126 [kg/s].

3 RESULTS

In order to analyze the fluid dynamical behavior of blood in the aorta without and with dissection, some control points and control lines in characteristic locations are defined (see Fig. 3 and Fig. 4). The control points and lines provide meaningful information corresponding the related variables like the volume fraction of RBCs and the velocity of blood. Since 3D computational domains are used, all points are placed approximately in the center of the aorta and the dissections. The control lines cross the geometry close to its axis.

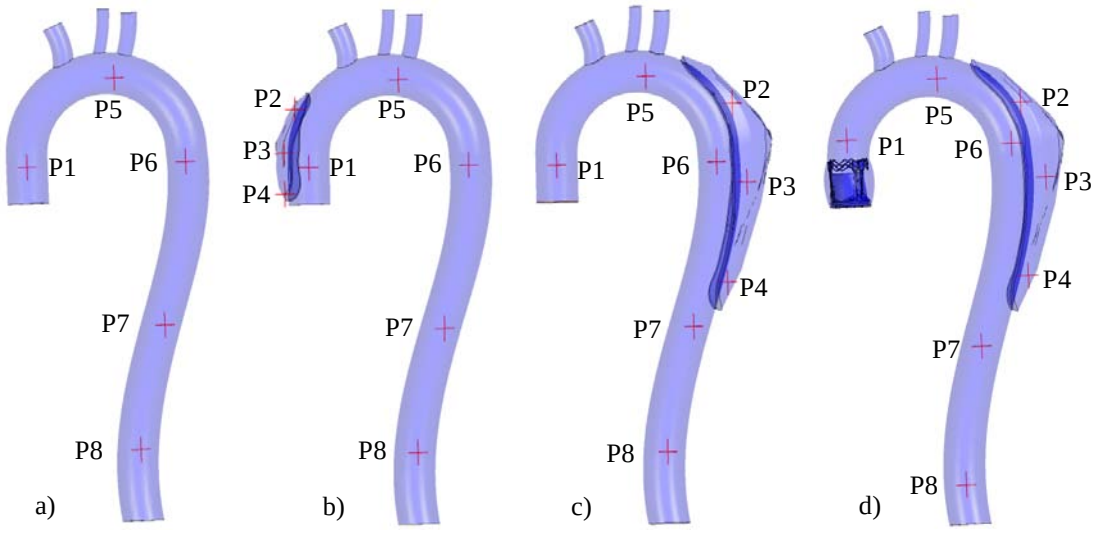

Figure 3: The control points chosen in the aorta: a) without dissection, b) dissection Stanford A, c) dissection Stanford B and d) dissection Stanford B with the implanted heart valve prosthesis.

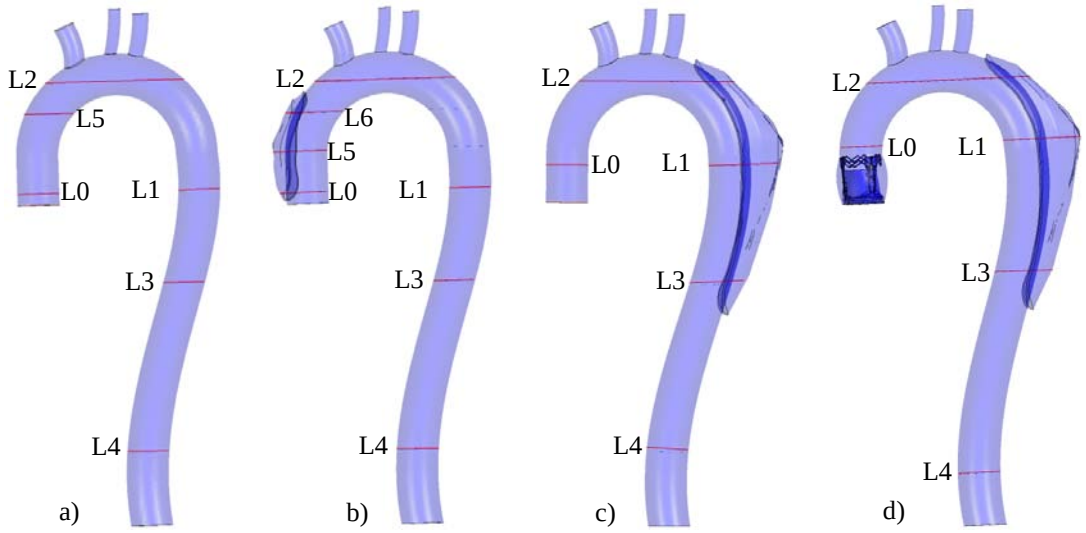

Figure 4: The control lines chosen in the aorta: a) without dissection, b) dissection Stanford A, c) dissection Stanford B and d) dissection Stanford B with the implanted heart valve prosthesis.

3.1 RBC volume fraction

During the numerical simulation, important changes of the RBC volume fraction are observed in the whole domain. The variations of the volume fraction denote inhomogeneous transport of RBCs in the cardiovascular system. Because the viscosity function was coupled not only with the shear strain rate field, but also with the hematocrit content, the fluid dynamic behavior of blood is affected also by the RBC volume fraction.

Figures 5 - 8 exemplify the volume fraction development in some control points within 5 s of numerical simulation. All diagrams indicate that the volume fraction patterns are stable close to the inlet (see P 1) from the second cycle. However, the content of RBCs changes dynamically in further control points. Especially, a continuous and asymptotic increase of the volume fraction in the lower part (P 4) and the decrease in the lower part of the dissection is clearly seen (P 2). The heart valve prosthesis contributes to the faster separation and sedimentation of RBCs in the dissection (Fig. 8).

The most stable content of the RBC volume fraction along the control line is close to the inlet of the aorta. Other control lines show very inhomogeneous distribution of RBCs. In the aorta without dissection, (Fig. 9, 10 and 11) it can be seen that the stroke volume influences stronger the RBC distribution than the initial volume fraction of RBCs. The difference in the initial volume fraction can be recognized first of all from the shifted curves. Generally, it can be stated that in the control lines of the aorta without dissection the volume fraction varies between 20 % and 70 %.

In comparison to the results for the aorta without dissection, Fig. 12 and Fig. 13 illustrate a significant difference of the RBC distribution. The characteristic increase of the RBC volume fraction up to almost 100 % in both dissections is registered. It is visualized by the control line L 0 in the case of type A and the control line L 3 for the dissection type B. In the upper part of dissection, the RBC volume fraction converges to zero, e.g. L 2 in Fig. 13.

Additionally, the influence of the heart valve prosthesis can be studied in Fig. 14. The heart valve changes the stable RBC distribution in the vicinity of the inlet (see L 0). The values close to the valve increase locally even up to 80 %.

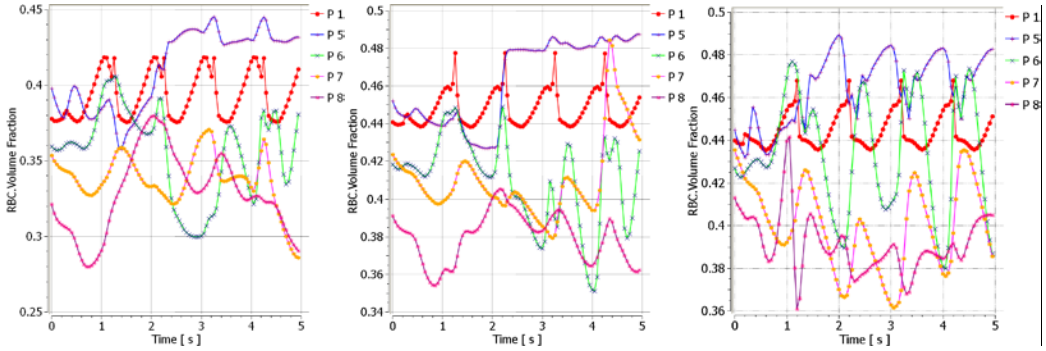

Figure 5: The RBC volume fraction in the aorta without dissection for 38 % hematocrit and 70 ml stroke volume (left), 44 % and 70 ml (middle) and 44 % and 120 ml (right).

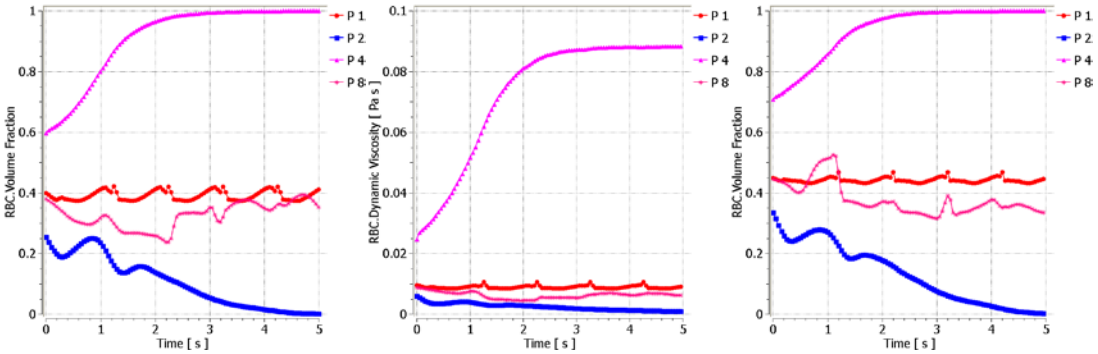

Figure 6: The RBC volume fraction in four control points of the aorta with dissection type A for 38 % hematocrit and 70 ml stroke volume (left), 44 % and 70 ml (middle) and 44 % and 120 ml (right).

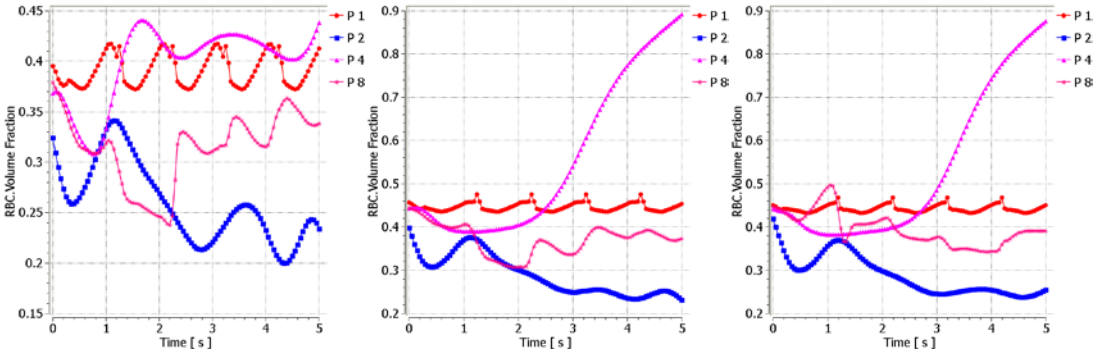

Figure 7: The RBC volume fraction in four control points of the aorta with dissection type B for 38 % hematocrit and 70 ml stroke volume (left), 44 % and 70 ml (middle) and 44 % and 120 ml (right).

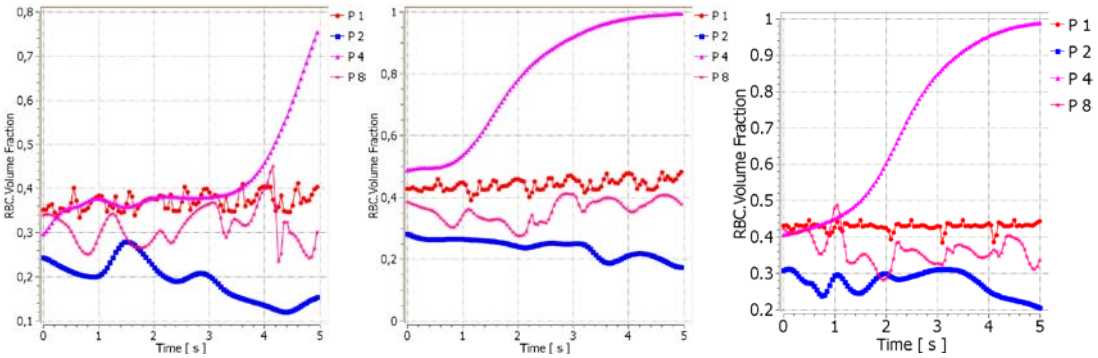

Figure 8: The RBC volume fraction in four control points of the aorta with dissection type B with the heart valve prosthesis for 38 % hematocrit and 70 ml stroke volume (left), 44 % and 70 ml (middle) and 44 % and 120 ml (right).

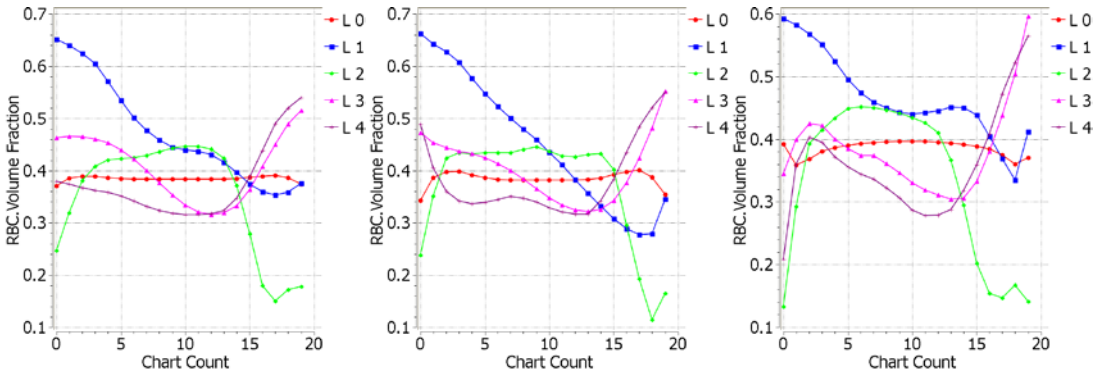

Figure 9: The volume fraction distribution on the control lines for 38% RBC and 70 ml stroke volume after 4.25, 4.5 and 5.0 s in the aorta without dissection.

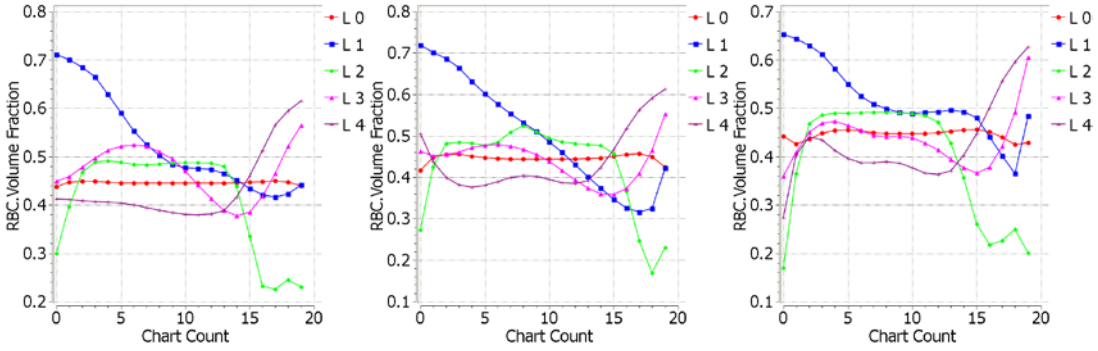

Figure 10: The volume fraction distribution on the control lines for 44% RBC and 70 ml stroke volume after 4.25, 4.5 and 5.0 s in the aorta without dissection.

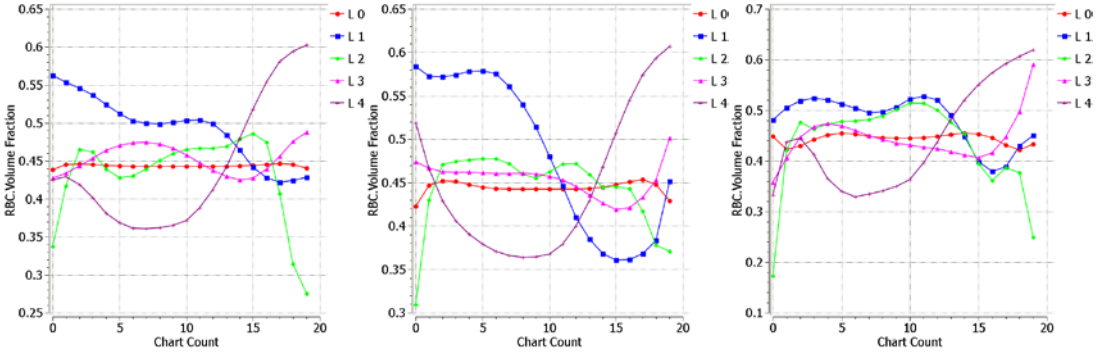

Figure 11: The volume fraction distribution on the control lines for 44% RBC and 120 ml stroke volume after 4.25, 4.5 and 5.0 s in the aorta without dissection.

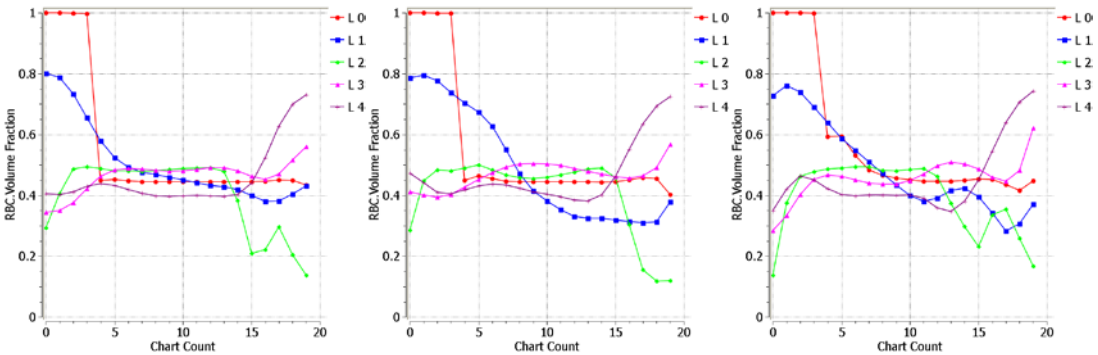

Figure 12: The volume fraction distribution on the control lines for 44% RBC and 70 ml stroke volume after 4.25, 4.5 and 5.0 s in the aorta with the dissection type A.

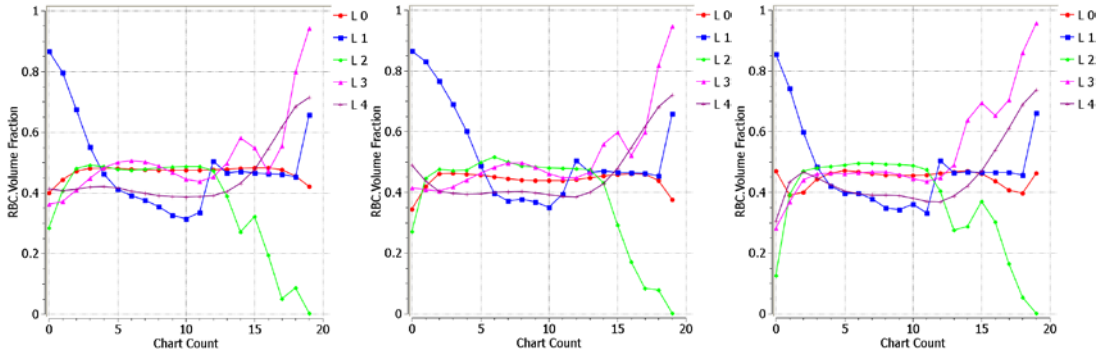

Figure 13: The volume fraction distribution on the control lines for 44% RBC and 70 ml stroke volume after 4.25, 4.5 and 5.0 s in the aorta with the dissection type B.

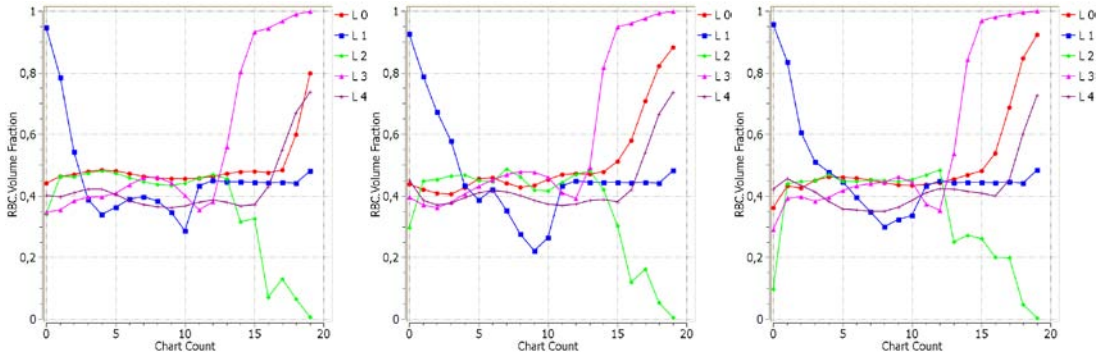

Figure 14: The volume fraction distribution on the control lines for 44% RBC and 70 ml stroke volume after 4.25, 4.5 and 5.0 s in the aorta with the dissection type B and the heart valve prosthesis.

3.2 RBC velocity

The velocity of RBCs in the aorta is affected by the systole and diastole phase. Figures 15 - 18 illustrate the blood velocity in some characteristic points in the aorta. Especially for the aorta without dissection, these velocity profiles are associated very close with the boundary condition applied at the inlet (Fig. 2). It is characterized by the fast velocity increase up to approx. 0.15 m/s for the volume stroke 70 ml and 0.25 m/s for the volume stroke 120 ml during the systole phase and almost zero velocity close to the inlet in the diastole. In the most cases the velocity profile stabilizes after the third cycle. Motion of the pressure wave can be derived from the differences between maximum velocities indicated at the top of the curves. The initial RBC volume fraction influences first of all the velocity profiles registered in the diastole phase. Similar effects are caused by both dissections. Furthermore, they induce more unstable flow in the descending aorta (P 6, P 7 and P 8). There are no considerable differences of the velocity curves in the true lumen for the aorta with dissection type A and B.

The additional implementation of the heart valve prosthesis leads to higher maximum velocity due to smaller cross sectional area of the inlet. The maximum velocity for the stroke volume of 70 ml reaches 0.19 m/s and for the stroke volume of 120 ml it amounts almost 0.4 m/s. Moreover, higher differences between the maximal velocities in the control points are observed. It indicates strongly modified wave motion characteristics in comparison to the cases without the heart valve prosthesis.

Considering the control points P 2, P 3 and P 4 in Fig. 16-18 the blood velocity distribution in dissections is studied. The results reveal substantial differences of the velocity in the false lumen in comparison to that in the true lumen. In the dissection the RBC velocity reaches 0.01 m/s.

The profiles presented in Fig. 19-24 illustrate velocity changes during systole and diastole phase along the control lines. The results illustrate following phases: the maximum point of systole 4.25 s, begin of diastole 4.5 s and the end of diastole 5.0 s. While in 4.25 s the forward blood flow can be seen in all control lines, the velocity alters its profile dramatically in 4.5 s when the heart valve is closing. The biggest difference at that time occurs between the ascending (L 0) and descending (L 1 and L 3) aorta. While in the descending part still forward blood flow with velocities of maximum 0.07 m/s can be seen, whereas the velocity close to the inlet in the middle of the ascending aorta reaches almost zero. At the end of diastole phase further decrease of the velocity can be stated. The significant drops of the RBC velocity in Fig. 22 (L 0) and Fig. 23 (L 1 and L 3) indicate values recorded in the false lumen. The implementation of the heart valve prosthesis contributes to the average increase of the blood velocity in all stages of the cycle by approx. 0.05 m/s, see e.g. Fig. 24.

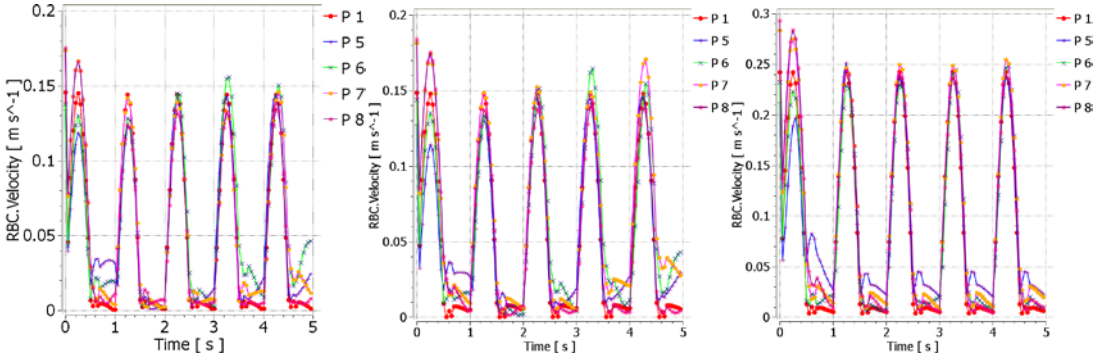

Figure 15: The RBC velocity in the aorta without dissection for 38 % hematocrit and 70 ml stroke volume (left), 44 % and 70 ml (middle) and 44 % and 120 ml (right).

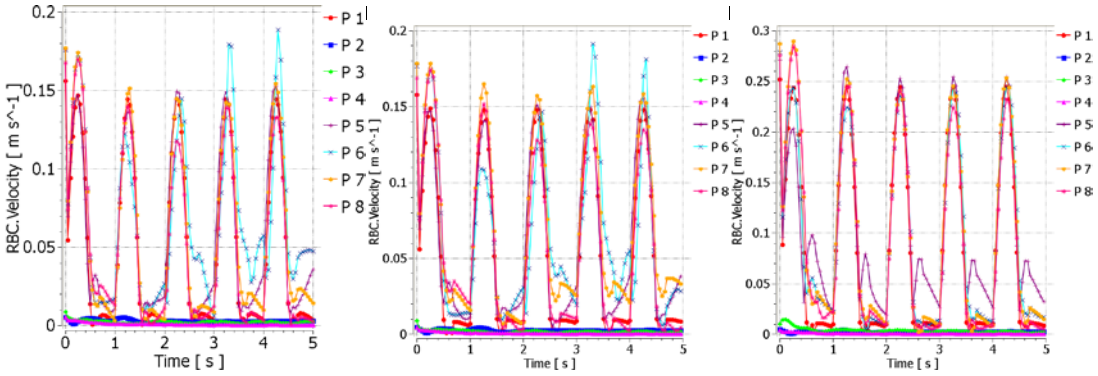

Figure 16: The RBC velocity in eight control points of the aorta with dissection type A for 38 % hematocrit and 70 ml stroke volume (left), 44 % and 70 ml (middle) and 44 % and 120 ml (right).

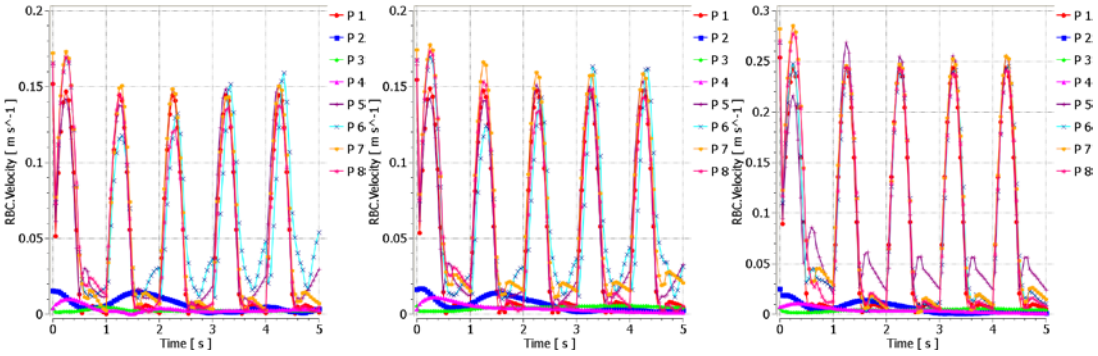

Figure 17: The RBC velocity in eight control points of the aorta with dissection type B for 38 % hematocrit and 70 ml stroke volume (left), 44 % and 70 ml (middle) and 44 % and 120 ml (right).

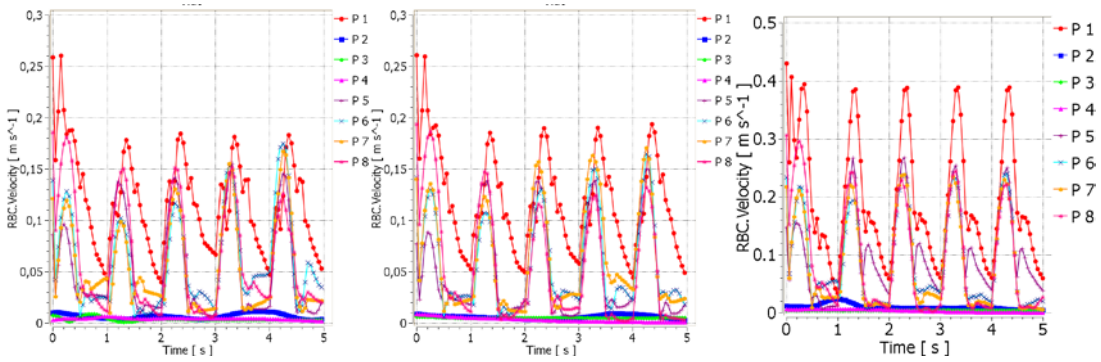

Figure 18: The RBC velocity in eight control points of the aorta with dissection type B with the heart valve prosthesis for 38 % hematocrit and 70 ml stroke volume (left), 44 % and 70 ml (middle) and 44 % and 120 ml (right).

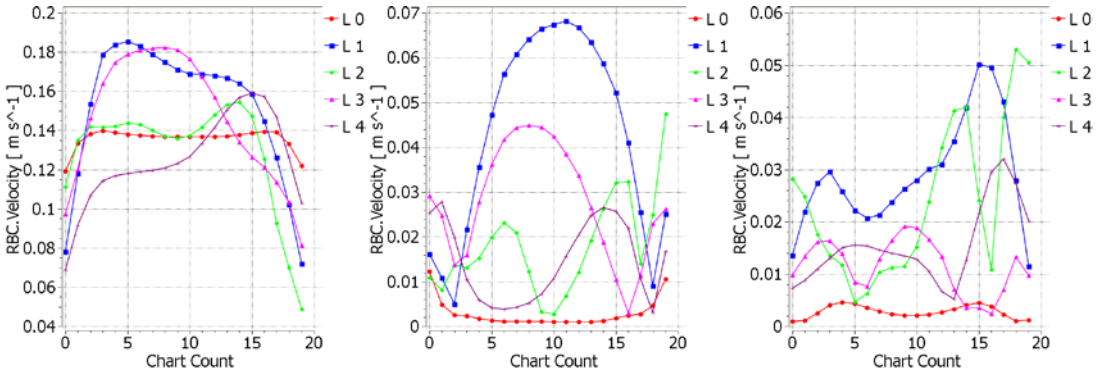

Figure 19: The velocity distribution on the control lines for 38% RBC and 70 ml stroke volume after 4.25, 4.5 and 5.0 s in the aorta without dissection.

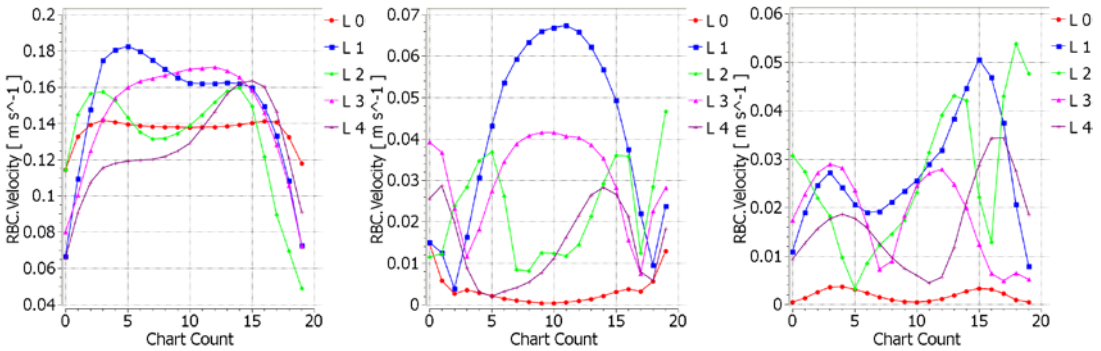

Figure 20: The velocity distribution on the control lines for 44% RBC and 70 ml stroke volume after 4.25, 4.5 and 5.0 s in the aorta without dissection.

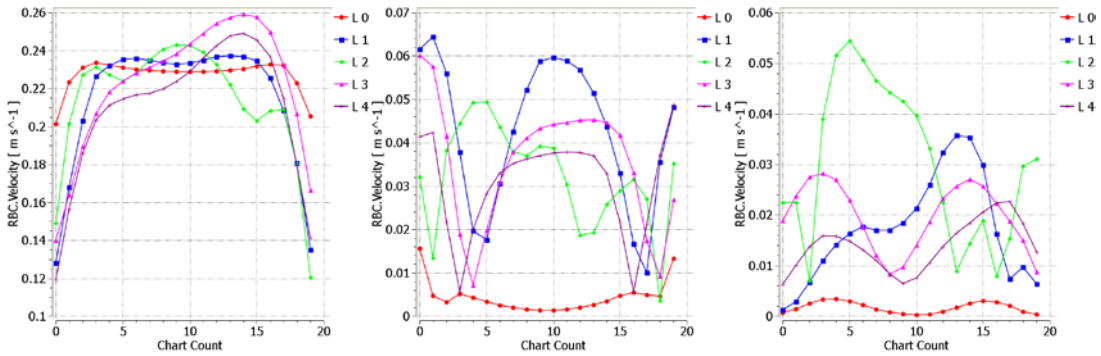

Figure 21: The velocity distribution on the control lines for 44% RBC and 120 ml stroke volume after 4.25, 4.5 and 5.0 s in the aorta without dissection.

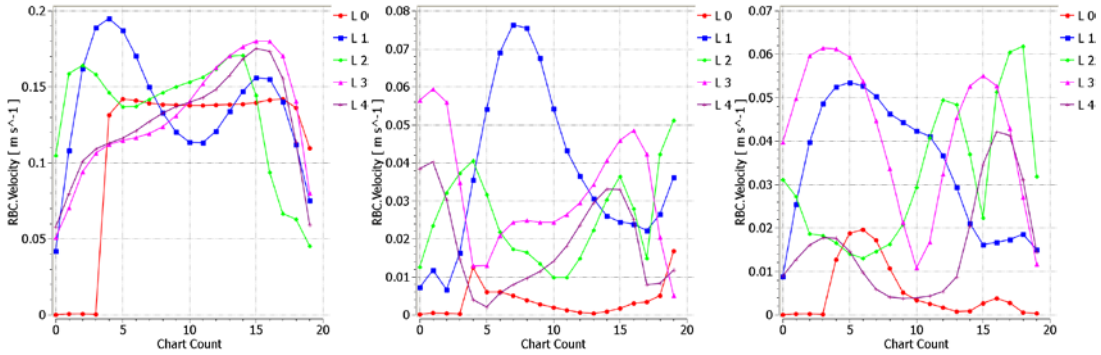

Figure 22: The velocity distribution on the control lines for 44% RBC and 70 ml stroke volume after 4.25, 4.5 and 5.0 s in the aorta with the dissection type A.

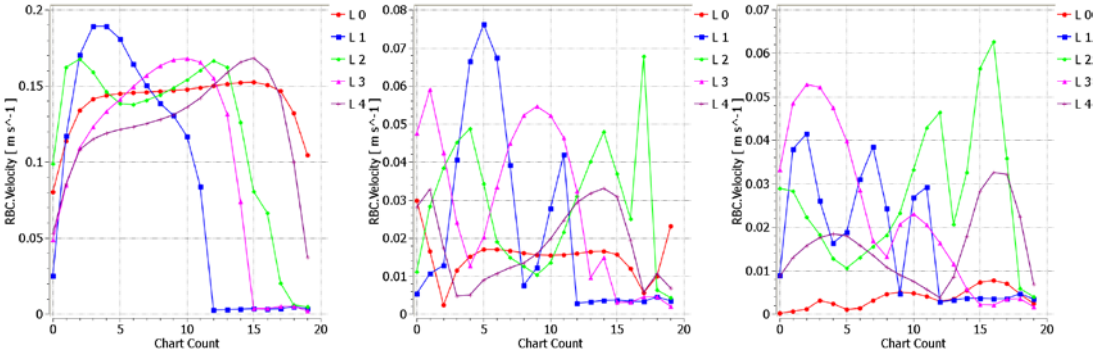

Figure 23: The velocity distribution on the control lines for 44% RBC and 70 ml stroke volume after 4.25, 4.5 and 5.0 s in the aorta with the dissection type B.

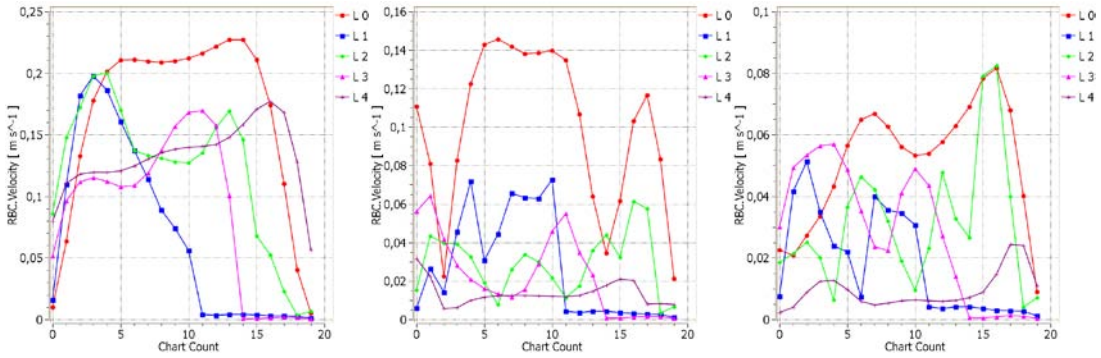

Figure 24: The volume fraction distribution on the control lines for 44% RBC and 70 ml stroke volume after 4.25, 4.5 and 5.0 s in the aorta with the dissection type B and the heart valve prosthesis.

3.3 Viscosity

The viscosity of blood is associated with the shear rate and the volume fraction of RBCs. In the main flow, it oscillates in the range of 0.004 ± 0.003 [Pa s]. Due to the increase of the RBC concentration in the lower part of dissections, the viscosity increases in this area 20 fold to about 0.08 [Pa s]. This value can be recognized at the asymptotical curve after 5 s of numerical simulation. It can be supposed that very high viscosity and the volume fraction of RBCs in this place induce thrombotic processes. Nevertheless, this behavior has to be verified by further numerical simulations and medical observations.

4 CONCLUSIONS

This paper shows the results of blood flow considered as a multiphase flow in the aorta without dissection, with dissection Stanford type A and B as well as dissection type B with the additionally implemented heart valve prosthesis. The main cognitions of this study can be summarized with following points.

- An inhomogeneous distribution of RBC volume fraction is observed in the aorta.
- The different initial RBC volume fraction influences the fluid dynamic behavior of blood especially in the diastole phase.
- The stroke volume affects both the velocity distribution and the RBC volume fraction distribution.
- There are significant differences in the hemodynamics observed in the false and true lumen.
- The RBC volume fraction in the dissection varies between 10 % at the top and 100 % at the bottom.
- The differences in the RBC volume fraction in the false lumen can contribute to thrombotic processes.
- The leukocytes do not influence significantly the hemodynamics in the aorta. Nevertheless, their presence in the multiphase flow should be considered to supply important information from the bio-chemical and medical point of view.
- The implementation of the heart valve prosthesis in the computational domain causes more physiological velocity profiles in the aorta.
- The heart valve prosthesis generates more inhomogeneous distribution of RBC volume fraction in the ascending aorta.

REFERENCES

[1] C.A. Taylor, M.T. Draney, Experimental and computational methods in cardiovascular fluid mechanics. *Annual Review of Fluid Mechanics* **36** pp. 197-231 (2004)

[2] D. Liepsch, An introduction to biofluid mechanics-basic models and applications. Journal of Biomechanics **35** pp. 415-435 (2002)

[3] D.N. Ku, Blood Flow in Arteries. *Annual Review of Fluid Mechanics*, **29** pp. 399-434 (1997)

[4] J.C. Lasheras, The Biomechanics of Arterial Aneurysms. *Annual Review of Fluid Mechanics* **39** pp. 293-319 (2007)

[5] D. Bessems, M. Rutten, F. van de Vosse, A wave propagation model of blood flow in large vessels using an approximate velocity profile function . *Journal of fluid mechanics*, 580 pp. 145-168 (2007)

[6] W. Fu, Z. Gu, X. Meng, B. Chu, A. Qiao, Numerical simulation of hemodynamics in stented internal carotid aneurysm based on patient specific model. *Journal of Biomechanics*, in Press (2010)

[7] K. Tsagakis, P. Massoudy, H. Jakob, Surgical techniques in acute type A dissection, *Zeitschr. Herz-, Thor- und Gefäßchirurgie* **23** pp. 335-344 (2009)

[8] K. Tsagakis, M. Kamler, H. Kuehl, W. Kowalczyk, P. Tossios, M. Thielmann, B. Osswald, P. Massoudy, T. Buck, H. Eggebrecht, H.G. Jakob, Avoidance of proximal

endoleakage using a hybrid stentgraft in aortic arch replacement and descending aorta stenting, *The Annals of Thoracic Surgery*, **88** pp. 773-779 (2009)

[9] U. Herold, K. Tsagakis, M. Kamler, P. Massoudy, E. Assenmacher, H. Eggebrecht, T. Buck, H. Jakob, Change of paradigms in the surgical treatment of complex thoracic aortic disease. *Herz* **31** pp. 434-442 (2006)

[10] H. Eggebrecht, U. Herold, O. Kuhnt, A. Schmermund, T. Bartel, S. Martini, A. Lind, C.K. Naber, P. Kienbaum, H. Kuhl, J. Peters, H. Jakob, R. Erbel, D. Baumgart, Endovascular stent-graft treatment of aortic dissection: determinants of post-interventional outcome. *European Heart Journal* **26** pp. 489-497 (2005)

[11] H. Eggebrecht, C.A. Nienaber, M. Neuhauser, D. Baumgart, S. Kische, A. Schmermund, U. Herold, T.C. Rehders, H.G. Jakob, R. Erbel, Endovascular stent-graft placement in aortic dissection: a meta-analysis. *European Heart Journal* **27** pp. 489-498 (2006)

[12] H. Kusagawa, T. Shimono, M. Ishida, T. Suzuki, F. Yasuda, U. Yuasa, K. Onoda, I. Yada, T. Hirano, K. Takeda, N. Kato, Changes in false lumen after transluminal stent-graft placement in aortic dissections - Six years' experience. *Circulation* **111** pp. 2951-2957 (2005)

[13] W. Kowalczyk , K. Tsagakis, D. Wendt, S. von Sobbe , A. Najafi, B. Kipfmüller and H. Jakob, Experimental and numerical investigation of a fluid flow in a model ascending aorta with dissection. *Minim Invasiv Ther*. **17** pp. 229–230 (2008)

[14] D. Wendt, M. Thielmann, T. Buck, R.-A. Jánosi, T. Bossert, N. Pizanis, M. Kamler and H. Jakob, First clinical experience and 1-year follow-up with the sutureless 3F-Enable aortic valve prosthesis, *Eur J Cardiothorac Surg* **33** pp. 542-547 (2008)

[15] ANSYS CFX Theory Guide Release 12.0 (2009) ANSYS, Inc.

[16] J. Jung, A. Hassanein, Three-phase CFD analytical modeling of blood flow, *Medical Engineering & Physics* **30** pp. 91-103 (2008)

[17] F.R. Menter, Zonal two equation $k-\omega$ turbulence models for aerodynamics flows. AIAA Paper 93-29006 (1993)

[18] S. Middelmann, Transport phenomena in the cardiovascular system, Wiley, New York (1972)